Int. J. Heat Mass Transfer. Vol. 21, pp. 193–201. Pergamon Press 1978. Printed in Great Britain

EXPERIMENTAL TEMPERATURE DISTRIBUTION AND HEAT LOAD CHARACTERISTICS OF ROTATING HEAT PIPES

T. C. DANIELS
Department of Mechanical Engineering, University College of Swansea, U.K.

and

R. J. WILLIAMS
NASA–Ames Research Center, Moffet Field, CA, U.S.A.

(*Received* 6 *December* 1976 *and in revised form* 27 *April* 1977)

Abstract—Experimental results show conclusively that the presence of a small quantity of a non-condensable gas (NCG) mixed with the working fluid has a considerable effect on the condensation process in a rotating heat pipe. The temperature distribution in the condenser shows the blanketing effect of the NCG and the ratio of the molecular weight of the working fluid to that of the NCG has a very definite effect on the shape of this distribution. Some of the effects are quite similar to the well-established data on stationary heat pipes.

NOMENCLATURE

θ_s, temperature difference between saturation temperature t_s and condenser wall temperature t_w;
Q_{local}, heat-transfer rate;
h_{f_g}, enthalpy of vaporisation or latent heat;
ρ, density of the working fluid;
k, thermal conductivity of the working fluid;
μ, viscosity of the working fluid;
σ, surface tension of the working fluid.

1. INTRODUCTION

IN RECENT years considerable interest has been generated in regard to the heat pipe as a heat transfer device. Attention has mainly been devoted to the stationary heat pipe which relies on capillary action for the recycling of the working fluid. In addition to its effective high thermal conductivity the stationary heat pipe has been proved to have excellent thermal control characteristics through the use of non-condensable gas. The capillary heat pipe however has a number of limitations such as the wicking limit, nucleate boiling etc., and some of these limitations can be overcome in a rotating heat pipe.

The rotating heat pipe is a closed hollow shaft with a slight internal taper along its axial length and contains a fixed amount of working fluid (Fig. 1). Heat is transferred from the evaporator to the working fluid causing evaporation. The vapour flows axially towards the condenser where it is condensed on the cooled walls. It is then centrifuged back to the evaporator along the tapered walls. The limitations imposed by the failure of a wick structure are therefore eliminated by the use of the centrifugal force field to return the condensate to the evaporator.

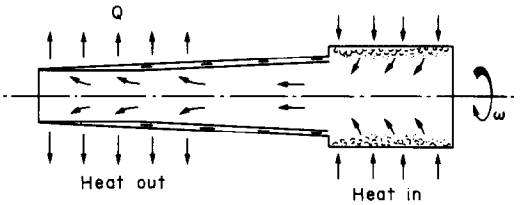

FIG. 1.

The experimental and theoretical analysis of rotating heat pipes has been concerned with their operation with pure vapour only [1] and yet experiments by Marto [2] indicate that inadequate filling procedures which fail to remove all the non-condensable gas, such as air, have a marked effect on the performance of the system.

With this in mind an experimental evaluation of the performance of the rotating heat pipe with non-condensable gases present was undertaken which would enable the migration of the non-condensable gas to be studied and to investigate the heat removal from the condenser.

2. EXPERIMENTAL APPARATUS AND PROCEDURE

The main components and general arrangement of the rotating heat pipe can be seen in (Fig. 2). The evaporator comprised a 76 mm-O.D. copper tube of wall thickness 3 mm and overall length 150 mm. At the outset a strong influence in the design of the apparatus was the ability to visually observe the inside of the heat pipe and to measure the temperature distribution inside the pipe itself. It was felt that by linking visual observations and experimental measurements a better understanding of the operation of the rotating heat pipe

could be obtained. A flange on the end of the evaporator enables an interchange between a toughend glass window for the visual observations and a travelling thermocouple probe for temperature measurement.

The evaporator was helically wound over 130 mm with a pyrotenax heating cable, thus providing an intended adiabatic section of 20 mm.

The condenser was machined from a thick walled cylindrical copper casting and was brazed to the evaporator. The condenser tapers from 63.7 to 37 mm over a length of 255 mm thus producing a half cone angle of 3° and a step at the condenser–evaporator intersection which allows the condensate to form a parallel liquid annulus in the evaporator (Fig. 2).

Thermometer where the temperature was read directly to an accuracy of $\pm 0.1\% \pm 0.5$°C with a resolution of 0.1°C per division. Initial checks were made to ensure that all the thermocouples recorded the same readings when the rig was in both stationary and rotating mode before any heat was applied to the heat pipe. There was no evidence of any significant e.m.f.'s being generated at the slip rings.

The following experimental procedure was used throughout the tests. The heat pipe was thoroughly cleaned using trichlorethylene and washed out with triple distilled water and then pumped down to a vacum of 5×10^{-3} torr. The non-condensable gas bled in first through a system of valves and a Pirani vacuum gauge

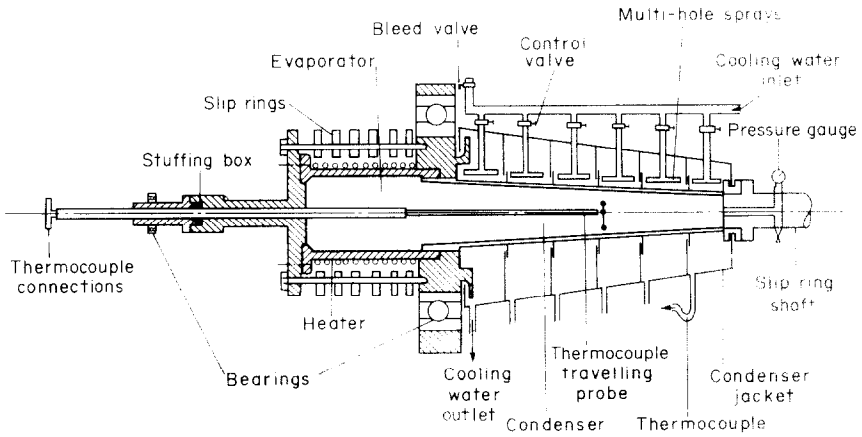

FIG. 2. Schematic diagram of rotating heat pipe.

In order to make an assessment as to what portion of the condenser would be used to transfer the heat in the case where non-condensable gases are present it was decided to segment the condenser. Hence it would be possible to focus more attention on local condensation rates and condenser wall temperatures. With a segmented condenser it would be possible to assess the influence of external cooling conditions and locate the region where the bulk of the heat was transferred. The condenser was therefore divided into six compartments and provision made in each one to record inlet and outlet cooling water temperatures, condenser wall temperatures and cooling water flow rates. Additional instrumentation consisted of two thermocouples embedded in the evaporator wall and one suspended in the evaporator vapour space. All the thermocouples were made with nickel chrome/nickel aluminium (Cr/Al) wire. The travelling thermocouple probe is shown in (Fig. 2). One of the three thermocouples employed in the probe was bent at right angles on to a radius of 18 mm, this gives a clearance of 0.5 mm between the thermocouple and condenser wall when the probe is in the "fully in" position. The other thermocouple was bent to a radius of 9 mm. The third thermocouple was left on the centre line of the condenser. The electrical signals from the rotating thermocouples were brought out through copper slip rings through a selector switch to a "Comark" Electronic

give the initial and final pressures with non-condensable gases within the system. A known volume of working fluid in liquid form would then be sucked into the heat pipe and sealed by valve closure on the heat pipe. When this filling procedure was complete the cooling water flow rate was adjusted to the required levels. As the surface area of each compartment decreases along the axial length of the condenser the cooling water flow rate in each compartment was set proportional to the area of that compartment so that the external cooling conditions were the same for each one. With this control over the coolant fluid it was possible to have constant wall temperature or constant heat flux. The heat pipe was slowly brought up to the required speed and power was supplied to the evaporator heater. Once thermal equilibrium had been reached all the rotating and stationary thermocouples and the pressure gauge was read and the water flow rates recorded. The travelling thermocouple probe was traversed along the length of the condenser, readings being taken at various stations. The power to the heater was then increased while the rotational speed was kept constant. The foregoing procedure was then repeated. This procedure was repeated for several heat inputs, rotational speed, working fluid and non-condensable gas combinations. This procedure was also repeated at selected conditions with the travelling probe replaced by the toughened glass window.

3. EXPERIMENTAL RESULTS

To assess the effect of a non-condensable gas on the operation of a rotating heat pipe it was essential to determine first the behaviour of the heat pipe when operated in the pure vapour state, i.e. no non-condensable gas present.

The pure vapour tests were carried out at three speed ranges, 600, 800 and 1000 rev/min which correspond to 15.4, 27.4 and 42.8 g at the entrance to the condenser test surface. For each speed a range the evaporator heat inputs employed was between 800 and 1400 W.

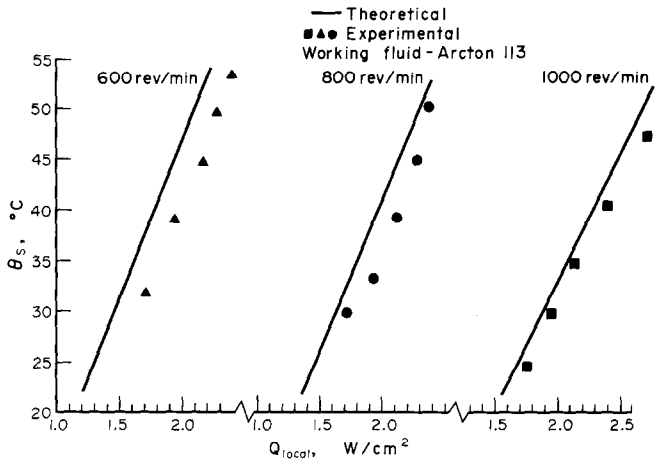

FIG. 3. Comparison of analytically predicted heat-transfer rates with experiments.

Good repeatability was obtained with all of the experimental data with approximately 80% of the heat input to the evaporator being recovered in the condenser cooling water. The 20% losses are probably due to conduction losses through the magnesium insulation, the probe support and condensation in the adiabatic section. However, further insulation of the rig would not have been feasible. The axial wall temperature distributions over the middle four compartments were uniform. The wall thermocouple reading in number one compartment nearest the evaporator however was a few degrees higher due to conduction down the wall from the evaporator. It is more convenient to discuss these wall temperature profiles in connection with those obtained with a non-condensable gas present.

Figure 3 shows the relashionship between the heat-transfer rates Q_{local} of the condenser and the temperature difference θ_s between the saturation temperature and condenser wall temperature. The figure shows good general agreement between experimental and theoretical results [3] and as explained earlier the wall temperature was constant over the middle four compartments and the variation in local heat flux being 5–8%. The theory [3] was based on a boundary-layer similarity type approach, the governing equations being numerically solved on a computer.

4. RESULTS OF VISUAL OBSERVATIONS

Visual observations were made by replacing the travelling thermocouple probe with the toughend glass window and repeating the runs at selected speeds and heat inputs. At each condition the evaporator and condenser performance was monitored with the aid of illumination from a strobe light.

In the evaporator at the low speed (600 rev/min) the boiling action was very violent with large vapour bubbles and a frothy liquid–vapour interface (the nucleation sites appeared to be clustered in various regions of the evaporator). By increasing the speed to 800 rev/min the bubble evolution in the evaporator was reduced due to the increased centrifugal force and produced a corresponding decrease in saturation temperature and pressure. The buoyancy effect on the vapour bubbles would be negligible at the value of "g" quoted earlier. It was observed that the boiling was much more uniform and controlled with smaller bubble diameters. These results correspond with the rotating boiler observations of Gray and Marto [4].

A phenomena indicated by the experimental results is that the rate of increase of heat transfer with rotational speed tends to fall off at a higher speed. Al-Jumaily [5] observed similar behaviour in his heat-transfer characteristics and put forward the following explanation: As the rotational speed increases the axial component of centrifugal force increases so that the film velocity will increase, hence there will be a tendency for a thinner film for a given flow rate. The resistance to the condensate flow is assumed to be influenced by the surface finish on the wall and this will, therefore, disturb the thinner, rather than the thicker layers. Consequently the circulation of the condensate maybe affected resulting in the inadequate removal of heat and the narrowing of the gap between the constant speed lines.

During experimental runs with three different fluid charges the condenser appeared mirror-smooth and shiny, which indicates that film condensation was occurring. On the other hand, the condenser appeared dull in colouration when rotated with no heat input.

It should be stated throughout the experimental programme several attempts were made to photograph the inside of the heat pipe during operation. While the

photographic results of the boiling process were partially successful, the inability to adequately light the inside of the condenser precluded any reasonable photographs being obtained.

5. RESULTS FOR ARCTON 113 WITH NITROGEN AS A NON-CONDENSABLE GAS

To explore the effect of a non-condensable gas on the operation of the heat pipe, tests were performed with various masses of nitrogen introduced into the system. Care was taken to ensure that the same external cooling conditions existed for these tests as for the pure vapour results.

In the results to be presented, two of the three variables (viz heat input, rotational speed, filling condition) will be kept constant while the third is varied.

6. EFFECT OF THERMAL LOADING ON HEAT INPUT

The effect of heat input on the condenser wall temperature profiles for a fixed rotational speed is shown in Fig. 4. They are plotted as the measured surface temperature of the condenser wall as a function of distance from the entrance of the condenser. The

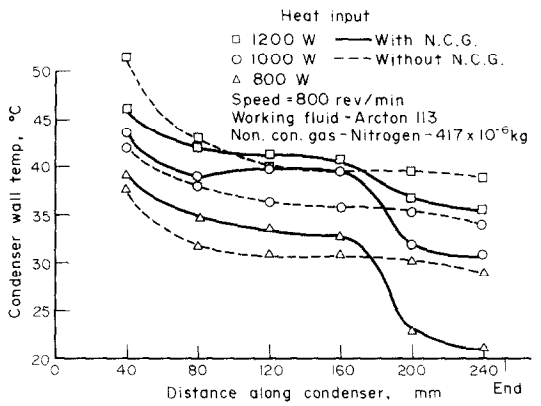

FIG. 4. Condenser wall temperature profile with and without non-condensable gas.

figures show the characteristic temperature distribution of the stationary non-condensable gas loaded heat pipe in that the higher temperature region is indicative of the active condenser. On the other hand, the low temperature region occurs where the condenser is gas blocked and inactive. The intermediate region of changing wall temperature indicates the vapour gas diffusion region. In the stationary gas loaded heat pipe an increase in heat input to the heat pipe has the effect of increasing vapour pressure and mass flow rate of the vapour and this in turn compresses the non-condensable gas thus moving the vapour gas diffusion front further down the condenser. In the case of the rotating heat pipe the vapour gas front does not significantly move down the condenser, the difference in temperature between the two regimes becoming less, thus smoothing out the step in the wall temperature profile. Physically this can be interpreted as either greater heat conduction down the condenser wall or the much heavier vapour at the higher pressures, forcing its way through the diffusion barrier provided by the non-condensable gas or a combination of both effects. The graph also shows the comparison of the wall temperature profiles for the case of the pure vapour. In general it can be seen that when non-condensable gases are present the heat is transferred at a higher temperature over the first part of the heat pipe—another similarity with stationary heat pipe operation.

These wall temperature profiles also give a good indication of the behaviour of the local heat flux along the condenser, i.e. the local heat flux falls along the length of the condenser in the same way as the temperature profile falls.

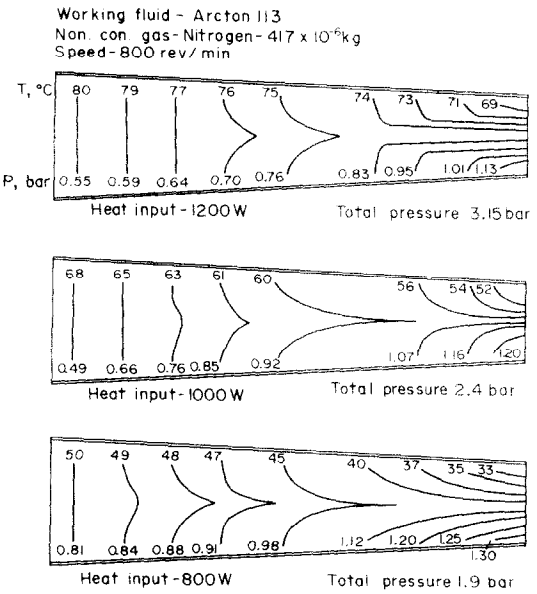

FIG. 5. Experimental isotherms and isobars—effect of heat input.

Figure 5 shows the internal isotherms and isobars obtained by traversing thermocouple probe along the entire length of the condenser. The temperature of the vapour gas isotherms are given along the top of each diagram while the pressure along the bottom corresponds to the partial pressures of the non-condensable gas. These were obtained by assuming that the components of the vapour gas mixture are perfect gases, thus enabling Dalton's Law to be used to calculate the partial pressures of both vapour and non-condensable gas. The isotherms in this figure are symmetrical about the centre line and decrease axially in magnitude along the condenser in a similar manner to the temperature profiles. Thus the partial pressure of the non-condensable gas increases towards the small end of the condenser, indicating a build-up of non-condensable gas at this end. The build-up of non-condensables also occurs in the radial direction. Both isotherms and isobars in this end section of the condenser are almost horizontal which suggests some sort of stratification or layering of the vapour gas mixture. The theoretical analysis assumed that there is a mixing of non-condensables and vapour in a radial direction and pre-

dicted a density variation and a build-up of NCG towards the interface. This is borne out by the above observations. The temperature profiles were built up from several traverses taking readings at very small distances apart. Only three radial thermocouples were used, an increase in the number would probably disturb the internal vapour flow too much. The centre line discontinuities of the isotherms may look severe but the difference between adjacent isotherms is only 2–3°C so that the radial temperature gradient is not as large as it looks. The isotherms are only meant to give an idea of what is happening inside the heat pipe.

From an examination of the three diagrams in (Fig. 5) several other factors are also evident. Firstly the temperature variation of the vapour gas mixture is greatest at the lower heat input (800 W) and the ratio of the partial pressure of non-condensable gas to the total pressure of the system is also greater, indicating a higher concentration of non-condensable gas. In addition, as the heat input is increased the vertical lines, which are indicative of pure vapour, are seen to advance further down the condenser. This behaviour is reasonable on physical grounds as an increase in heat input causes more vapour to be generated, thus decreasing the overall concentration of non-condensable gas. The accompanying increase in vapour mass flow rate forces the pure vapour front further down the condenser and this phenomena is more readily discernable from the isotherm plots than the wall temperature distributions discussed earlier.

7. EFFECT OF SPEED

The effect of speed on the condenser wall temperature profiles for a particular filling condition and heat input is shown in (Fig. 6). Increasing the speed has the same effect on the non-condensable gas case as the pure vapour, namely to reduce the wall temperature. This is attributed to the suppressed boiling phenomena reducing bubble evolution in the evaporator and thus decreasing saturation pressure and temperature. Similar trends have been observed by Al-Jumaily [6] and Gray [4]. In the 1000 rev/min profile there appears to be a more uniform decrease in temperature with no "step" from high to low temperature regions. This is probably due to the higher centrifugal force spreading out or layering the non-condensable gas along the liquid vapour interface and causing a blurring of this interface.

As would be expected the local heat flux profiles exhibit similar behaviour at the various speeds with little difference between the individual curves, since approximately the same amount of heat is being transferred in each case. A familiar pattern of internal isotherms is shown for the 800 and 1000 rev/min cases in Fig. 7 with the 600 rev/min diagram being greatly different. It has already been stated that increasing the speed has the effect of reducing the total pressure and temperature and the pure vapour front can clearly be seen in both the 800 and 1000 rev/min diagrams.

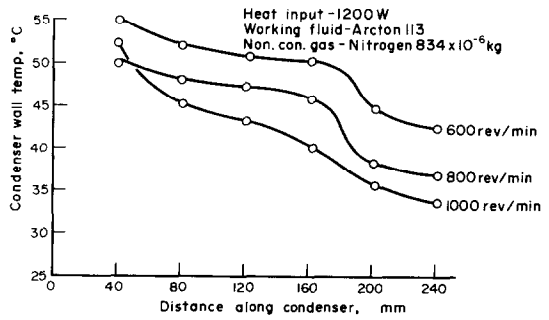

FIG. 6. Condenser wall temperature profiles—effect of speed.

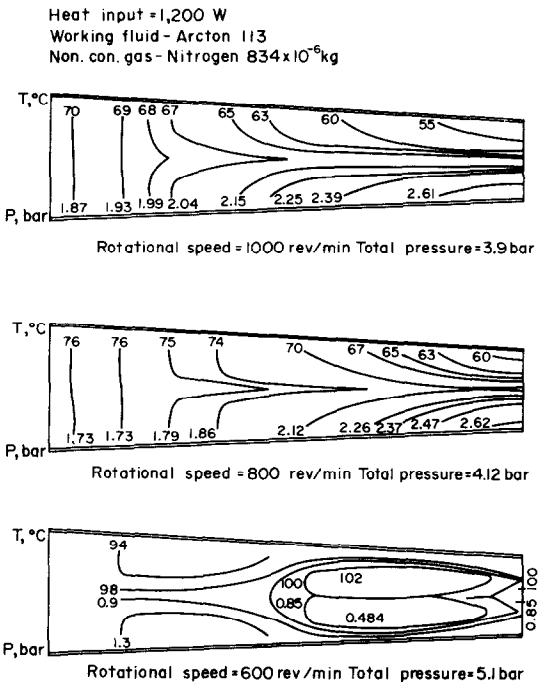

FIG. 7. Experimental isotherms for vapour–gas mixture and partial pressures lines for non-condensable gas.

The closed loop isotherms of the 600 rev/min case suggest stagnant pockets of vapour gas mixture, further experiments carried out at 600 rev/min produced isotherms which were generally unpredictable. However, this slow speed effect required much more experimental work to be carried out before it is fully understood.

8. EFFECT OF FILLING CONDITION

The rotating heat pipe was run with two different filling conditions for non-condensable gas. The mass of non-condensables present was again found by calculating its partial pressure after filling and then, by using the perfect gas law, the overall mass of non-condensables can be found. Figure 8 shows the condenser wall temperature profiles for the two conditions examined, together with the condenser wall temperature profile for the pure vapour case. The diagram shows that, as before, the introduction of a non-condensable gas has the effect of raising the condenser wall temperature over part of the condenser (so-called active part) and lowering the temperature over the end portion of the condenser where the non-condensables are concentrated. Increasing the overall mass of non-conden-

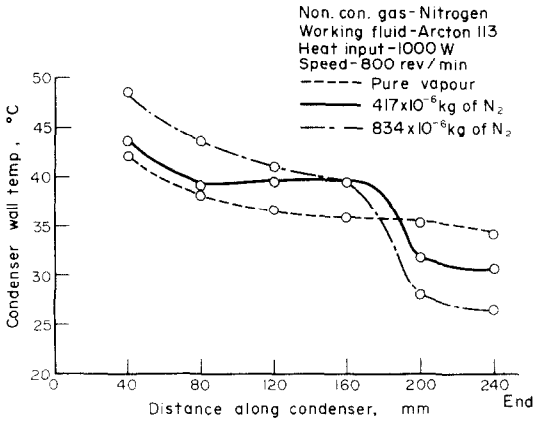

FIG. 8. Condenser wall temperature profiles.

sables in the system exaggerates these effects, i.e. higher temperature over initial part of condenser, lower temperature over final part of condenser.

The foregoing is now repeated for a different working fluid—acetone and non-condensable gas carbon dioxide.

9. PURE ACETONE VAPOUR RESULTS

Figure 9 shows the relationship between the temperature difference θ_s (saturation temperature minus the condenser wall temperature) and the heat transfer rates Q_{local} for the three speeds investigated. Experimental points again being the average of the middle

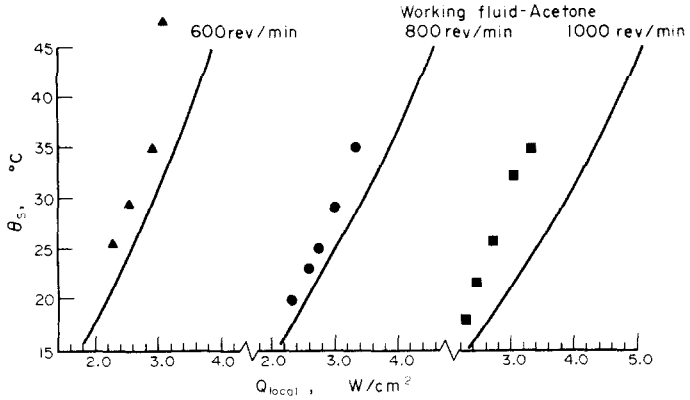

FIG. 9. Comparison of theoretical and experimental results for pure vapour.

four compartments. For this combination experimental points lie to the left of the theoretical results which indicates that the empirical heat-transfer coefficients are lower than expected. Similar trends have been observed by Lee and Mital [7] during the operation of a stationary, vertical closed thermosyphon. They found that their theory overestimates the heat-transfer rate for high merit number fluids such as water and underestimates the rate for low merit number fluids such as the Arctons. A merit number is a fluid property group defined by

$$\frac{\rho^2 h_{fg} K^3}{\mu}$$

[5, 6] for rotating heat pipes, or where σ and K are the surface tension and thermal conductivity of the working fluid.

$$\frac{\rho\sigma h_{fg}}{\mu}$$

for stationary heat pipes [8].

The diagram also shows that the increase in heat-transfer rate for the experimental points between the 800 and 1000 rev/min case is small which again indicates an upper limit in speed above which no increase in heat-transfer rate would be obtained as previously explained.

The wall temperature profiles were very uniform with a larger variation in local heat flux than in the Arcton 113 case (see comparison with non-condensable gas results in the next section).

10. ACETONE & CARBONDIOXIDE RESULTS

Effect of heat input

Figure 10 shows the effect on wall temperature profiles of introducing carbon dioxide (166×10^{-5}kg) into the system and the effect of heat input on the system. The figure shows that whereas with Arcton 113/N_2 two distinctive temperature regions existed, with acetone/Co_2 the wall temperature profiles appear to decrease at a uniform rate, levelling out towards the end of the condenser. This appears to be due to the mixing of the vapour and non-condensable gas since their molecular weights are not widely different, the vapour being unable to centrifuge effectively through the gas barrier. Thus producing a vapour–gas interface which existed over most of the length of the condenser with a greater layering or stratification of the two components. Increasing the heat input has the usual effect of increasing the condenser wall temperature whilst maintaining a similar profile.

The condenser local heat flux profiles behave in a similar manner, in each case approximately 75% of the total heat recovered in the cooling water being transferred in the initial two compartments of the condenser. However, mapping of the isotherms (see Fig. 11) shows that as the heat input was increased, the isotherms reverse their shape with the temperature decreasing towards the centre-line, while increasing towards the

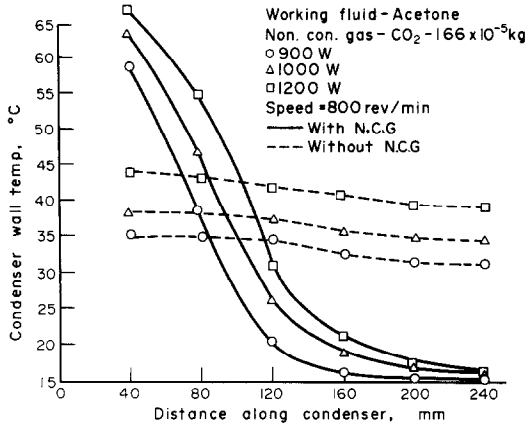

FIG. 10. Condenser wall temperature profiles.

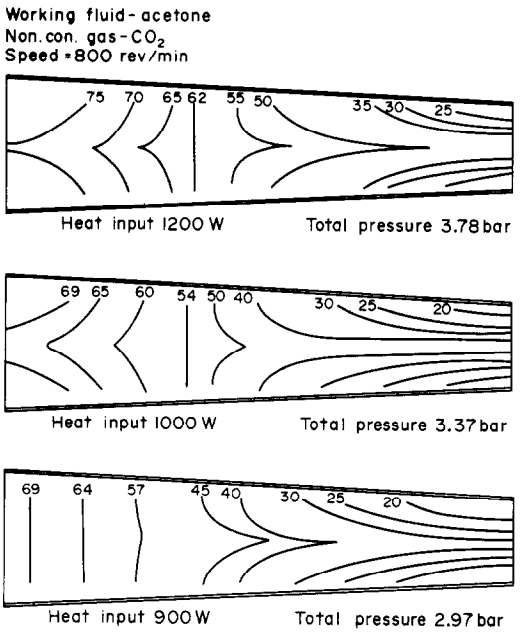

FIG. 11. Experimental isotherms—effect of heat input.

wall. It is over this section that 75% of the total heat load is being transferred. The non-condensable gas appears to be providing such an effective barrier to the vapour that more heat is transferred by conduction down the wall of the condenser causing a large variation in wall temperature as was shown in Fig. 10. However, for this to be substantiated experiments with either different condenser wall materials or increased instrumentation have to be carried out.

Effect of speed

The effect of speed on the condenser wall temperature profiles is not as pronounced as that for the Arcton 113/N_2 case of Fig. 6. However, the same format of experimental results exists, i.e. higher speed giving a lower wall temperature for the reasons already explained. The individual condenser heat flux profiles for the three speeds employed were again very similar to those of Arcton 113/N_2 with, as stated, approximately

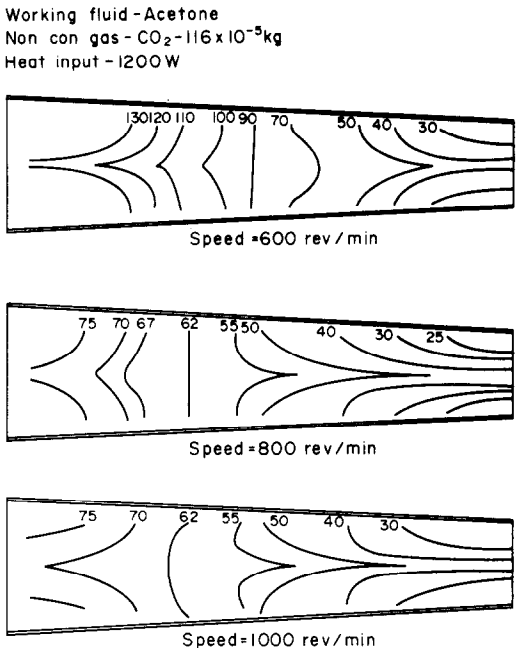

FIG. 12. Experimental isotherms—effect of speed.

75% of the heat being transferred in the first two compartments. However, the internal isotherms of Fig. 12 have several interesting features which were not present for the Arcton 113/N_2 tests. The vapour at the entrance to the condenser for the 600 rev/min case is superheated since all the fluid was boiled off in the evaporator, sufficient heat input being available to produce several degrees of superheat. The isotherms again display a reversal in direction with a temperature gradient of over 100°C along the length of the condenser. When the speed was increased to 800 rev/min the vapour gas mixture in the initial part of the condenser lost its superheat and the temperature dropped by approximately 50°C with a corresponding decrease in axial temperature gradient. Little difference exists between the 800 and 1000 rev/min results which again suggests this upper speed limit beyond which there is no apparent difference in the results. Furthermore as these two experimental runs were not consecutively carried out the similarity between the two is remarkable.

Effect of filling condition

The effect on the condenser wall temperature profile for the three filling conditions employed is shown in Fig. 13. Apart from the 332×10^{-6} kg of Co_2 condition the wall temperature profiles exhibit the same behaviour as the Arcton 113/N_2 case, increasing the overall mass of non-condensables producing a higher temperature in the initial part of the condenser and a lower temperature in the end portion of the condenser. With all profiles the "two temperature regime" is indistinct indicating a greater mixing of the two components with an associated larger conductive heat transfer down the condenser wall.

Comparing the internal isotherms of Fig. 14 with the wall temperature profiles of Fig. 13 it can be seen that the introduction of a small amount of non-condensable

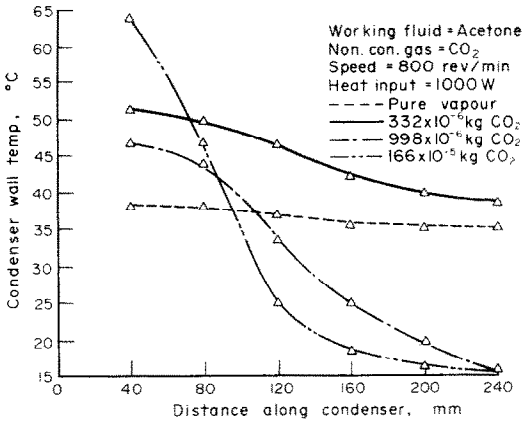

FIG. 13. Condenser wall temperature profiles.

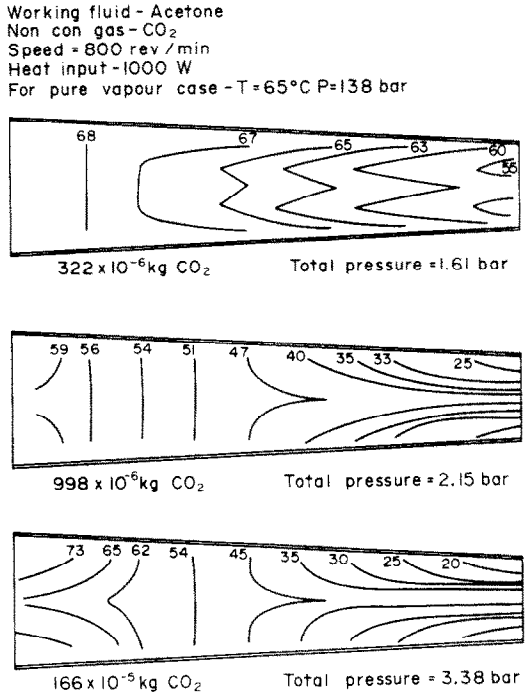

FIG. 14. Experimental isotherms for various filling conditions.

gas (332×10^{-6} kg) has the effect of raising the wall temperature along the entire length of the condenser, while the saturation temperature over the first two-thirds of the condenser is also higher than in the case of the pure vapour.

When the mass of non-condensables was increased to 998×10^{-6} kg the familiar shapes are again encountered. The saturation temperature relative to the pure vapour takes the expected form. The beginnings of the isotherm reversal trend can also be seen, while increasing the mass of non-condensables further to 166×10^{-5} kg exaggerates this with the isotherm reversal now plainly in evidence.

CONCLUSIONS

The foregoing experiments show conclusively that the presence of non-condensable gases have a considerable effect on the temperature distribution and the heat load characteristics of condensers of rotating heat pipes. Some of these effects are very similar to the published data on stationary heat pipes.

REFERENCES

1. T. C. Daniels and F. K. Al-Jumaily, Theoretical and experimental analysis of a rotating wickless heat pipe, in *Proceedings of the First International Heat Pipe Conference*. IKE-VDI, Stuttgart (1973).
2. P. J. Marto, Performance characteristics of rotating wickless heat pipes, in *Proceedings of the Second International Heat Pipe Conference*. Bologna, ESA, Noordwijk (1976).
3. R. J. Williams, Influence of inert gases on the performance of rotating heat pipes, Ph.D. Thesis, University College of Swansea, Wales (1976).
4. V. H. Gray, P. J. Marto and A. W. Joslyn, Boiling heat transfer coefficients, interface behaviour and vapour quality in a rotating boiler operating at 475 G's, NASA TN D4136 (March 1976).
5. T. C. Daniels and F. K. Al-Jumaily, Investigation of the factors affecting the performance of a rotating heat pipe, *Int. J. Heat Mass Transfer* **18**, 961–973 (1975).
6. F. K. Al-Jumaily, Investigation of the factors affecting the performance of a rotating heat pipe, Ph.D. Thesis, University College of Swansea, Wales (1973).
7. Y. Lee and U. Mital, A two-phase closed thermosyphon, *Int. J. Heat Mass Transfer* **15**, 1695–1707 (1972).
8. P. D. Dunn and D. A. Reay, *Heat Pipes*. Pergamon Press, Oxford (1976).

DISTRIBUTION EXPERIMENTALE DE TEMPERATURE ET CARACTERISTIQUES DE CHARGE THERMIQUE POUR LES CALODUCS TOURNANTS

Résumé—Des résultats expérimentaux montrent que la présence d'une petite quantité de gaz incondensable (NCG) mélangé au fluide vecteur a un effet considérable sur le mécanisme de condensation dans un caloduc tournant. La distribution de température dans le condenseur montre l'effet barrière du NCG et le rapport des masses moléculaires du fluide vecteur et du NCG a un effet très défini sur la forme de cette distribution. Quelques uns de ces effets sont très semblables aux résultats bien connus sur les caloducs fixes.

EXPERIMENTELLE TEMPERATURVERTEILUNG UND WÄRMELASTEIGENSCHAFTEN VON ROTIERENDEN WÄRMEROHREN

Zusammenfassung—Experimentelle Ergebnisse zeigen schlüssig, daß die Anwesenheit einer kleinen Menge nicht kondensierbaren Gases (NKG), vermischt mit dem Arbeitsmedium, eine beträchtliche Wirkung auf den Vorgang der Kondensation in einem rotierenden Wärmerohr hat. Die Temperaturverteilung im

Kondensator zeigt den bedeutenden Einfluß des NKG. Das Verhältnis des Molekulargewichts des Arbeitsmittels zu dem des NKG hat eine sehr bestimmte Wirkung auf die Form dieser Verteilung. Einige dieser Effekte sind den wohlbekannten Ergebnissen für stationäre Wärmerohre sehr ähnlich.

ЭКСПЕРИМЕНТАЛЬНОЕ ОПРЕДЕЛЕНИЕ РАСПРЕДЕЛЕНИЯ ТЕМПЕРАТУРЫ И ТЕПЛОВОЙ НАГРУЗКИ ВРАЩАЮЩИХСЯ ТЕПЛОВЫХ ТРУБ

Аннотация — Результаты эксперимента наглядно показывают, что небольшое количество неконденсируемого газа (НКГ), смешанного с рабочей жидкостью, существенно влияет на процессы конденсации во вращающейся тепловой трубе. Распределение температуры в конденсаторе свидетельствует о наличии эффекта покрытия НКГ, а отношение молекулярного веса рабочей жидкости к молекулярному весу НКГ оказывает вполне определенное влияние на вид этого распределения. Некоторые из эффектов очень схожи с хорошо известными результатами по стационарным тепловым трубам.